This is an Author Accepted Manuscript version.

Verification of Attitude Determination and Control Algorithms using Air-Bearing Test Table

Demet Cilden-Guler (http://orcid.org/ 0000-0002-3924-5422)[a,*], Aykut Kutlu[b] and Chingiz Hajiyev (http://orcid.org/ 0000-0003-4115-341X)[c]

[a] *Department of Astronautics Engineering, Istanbul Technical University, Istanbul, Türkiye*

[b] *Esen System Integration, Ltd., Ankara, Türkiye*

[c] *Department of Aeronautics Engineering, Istanbul Technical University, Istanbul, Türkiye*

**e-mail: cilden@itu.edu.tr*

Abstract— A test platform is developed to provide experimental verification of attitude and control algorithms for a satellite. The testbed is used for the development and implementation of test cases including sensors, actuators, and algorithms. The sensor suite consists of magnetometers, accelerometers, and gyroscopes used for state estimation. Three reaction wheels are used on each axis as the primary attitude control actuator. The test setup consists of the main payload-carrying table, mass balancing blocks, adapters for equipment installation, in order to make the mass balance, coarse balancing blocks are placed on the four corners and fine ones are mounted on each principal axis. The platform has a wireless monitoring system and a power distribution unit for online analysis. A computer is used to manage attitude determination and control tasks in a distributed control mechanism. After testing the maneuverability of the control system, various scenarios are evaluated and analyzed for magnetometer calibration and for satellite attitude estimation using traditional and nontraditional Kalman type filters.

Keywords: attitude determination and control, sensor calibration, spacecraft, air-bearing, test platform

1. INTRODUCTION

Attitude Determination and Control System (ADCS) algorithms [1, 2] can be adopted using computer software, and must be validated in an appropriate test configuration. Research suggests ground verification methods for evaluating designed algorithms before spacecraft launch, with the ADCS being a challenging subsystem to test in disturbance-free rotations [3–8].

A ground test system for attitude determination and control of a satellite is presented in many studies [9–12]. The most widely used simulator platform for spacecraft rotational dynamics is based on air bearings as stated in [3]. The air-bearing platform is used to advance the satellite model by providing practically torque-free rotating motion. Torque disturbances are primarily produced by the environment, platform, static and dynamic imbalance torques, and torques due to vibrations and electromagnetic interaction [7]. These torques can be eliminated in the design stage or by active systems. Orbit and attitude estimator is implemented on a closed-loop simulator with a ground test environment based on a real spacecraft flight data in [13]. A spin magnetic attitude control system is validated using an air-bearing experiment table in [14]. In the hardware-in-the-loop experiment (HIL), only magnetic rods are used as attitude actuators as six sets of two rods. An experimental setup with a ball and wheel system is used in [15] for verifying the control algorithms. ADCS

actuators with a quick response to generate an active momentum modifies the satellite attitude. The work in [16], a speed PID controller is designed for a reaction wheel using low-cost materials for its implementation in 1U CubeSats. A study in [17] describes a hardware design of a tilted wheel and its experimental setup as standalone and on a spherical air-bearing table. A benchmark is tested on three microprocessors through performance analysis of output power consumption in [18] in the context of attitude determination and control. Attitude control methods based on feedback linearization and state-dependent Riccati equation for a satellite are assessed using a frictionless spherical air-bearing test platform in [19]. Attitude control algorithms for fault diagnosis, prediction, and tolerant control are verified using a platform in [20]. Another study for spacecraft attitude control testing when maneuvering at a large angle is carried out on three-axis air-bearing testbed using a joint actuator including flywheel, thruster, and automatic balancing device in [21].

An air-bearing attitude simulator is used in [5] with reaction wheels as actuators, magnetometers, and sun sensors as attitude sensors. The extended Kalman filter (EKF) algorithm is verified using the test table on estimating the attitude states with the aid of the initialization information from one of the single-frame algorithms, QUEST.

This study develops adjusting algorithms for HIL in laboratory conditions using low friction motion on an air-bearing table with unconstrained rotation and constrained tilt angles [22]. First, the maneuvering capability of the platform using the control algorithms is tested. Furthermore, traditional-based and one of the single-frame methods based Kalman-type filtering algorithms [23, 24] are validated using the test platform. A magnetometer calibration is also presented in case of a possible fault on the magnetometer measurements.

The remainder of the paper is organized as follows. Section 2 presents the structural design and assembly of the test setup. The introduction of equipment that functions as sensors and actuators (reaction wheels) with attitude determination and closed-loop control system software is carried out in Section 3. In Section 4, the algorithms are validated on the test setup. The last section concludes the paper.

2. DESIGN AND ASSEMBLY OF THE TESTBED

In this section, the design and assembly of the test setup and the system architecture are given. Closed-loop control loops and PC-104 hardware are used as the Real-Time Central Processing Unit Computer, which run all algorithms and manage the entire system. With this computer, which is suitable for rapid prototyping, the algorithms and models prepared in the Matlab/Simulink environment are directly translated into C language and run on this computer in real-time.

3-axis Inertial Measurement Unit (IMU) is used to measure the attitude and angular rate of the system. The system consists of a microelectromechanical systems-based set of sensors, including a 3-axis rate gyroscope, accelerometer, and magnetometer. The test table weighs 22.6 kg and has a 70 cm outer circular diameter and 0.8 cm thickness. The main equipment includes sensors/IMU, reaction wheels, and modem, with a computer at the center and a battery block at the bottom. It is located in the power distribution box, which is symmetrical in terms of coarse mass balance.

3. ATTITUDE DETERMINATION AND CONTROL SYSTEM SOFTWARE

The ADCS model is created in the Matlab/Simulink environment. This model was converted to C language using the Matlab Real Time XpC Target tool and is utilized on the air bearing main control computer.

The Matlab/Simulink-based attitude determination and control system model comprises of the modules described below:

- Air bearing table with dynamic and kinematic mathematical models,
- Attitude control algorithm (Proportional, Derivative (PD) controller),
- Reaction wheel mathematical model (based on U7 motor parameters),
- Attitude estimation algorithms,

- Magnetometer calibration algorithm,
- Attitude error calculator.

The goal of this architecture is to demonstrate the maneuverability of the wheels and the performance of the estimation algorithms.

First, we present the kinematic model for a rigid body using the quaternion attitude representation as [9],

$$\dot{\boldsymbol{q}}(t) = \frac{1}{2}\Omega(\boldsymbol{\omega}_{BN}(t))\boldsymbol{q}(t) \tag{1}$$

Here, $\boldsymbol{q}$ is the quaternion vector, $\boldsymbol{q} = \begin{bmatrix} q_1 & q_2 & q_3 & q_4 \end{bmatrix}^T$. First three of the terms represent the vector part and the last one is the scalar term, with $\boldsymbol{q} = \begin{bmatrix} \boldsymbol{g}^T & q_4 \end{bmatrix}^T$ and $\boldsymbol{g} = \begin{bmatrix} q_1 & q_2 & q_3 \end{bmatrix}^T$. $\Omega(\cdot)$ is the skew-symmetric matrix, $\boldsymbol{\omega}_{BN} = \begin{bmatrix} \omega_x & \omega_y & \omega_z \end{bmatrix}^T$ is the body angular rate vector with respect to the inertial frame. The reference frame and the body frame are presented in Fig. 3. The dynamic equations of the satellite's rotational motion can be derived based on the Euler's equations;

$$\mathbf{J}\frac{\boldsymbol{\omega}_{BN}}{dt} = \boldsymbol{N}_d - \boldsymbol{\omega}_{BN} \times \left(\mathbf{J}\boldsymbol{\omega}_{BN}\right), \tag{2}$$

where $\mathbf{J}$ is the mass moment of inertia matrix which consists of principal moments of inertia as $\mathbf{J} = diag\left(J_x, J_y, J_z\right)$ and $\boldsymbol{N}_d$ is the vector of disturbance torque affecting the satellite. The external magnetic field effects are not considered in this study. The disturbance torque is assumed a constant value.

The block diagram of attitude determination and control algorithms to be tested on the platform are presented in Fig. 4. The attitude and angular velocity estimation can be obtained from a conventional Kalman-type filter or SFM-aided Kalman-type filter. Therefore, the connecting lines of the estimation algorithms in Fig. 4 are dotted lines.

The single frame-methods aided Kalman type filters are designed as two stages. In the beginning, one of the single-frame methods processes the theoretical models and the measurements and provides attitude measurements to the second stage. At least two vectors need to be measured in order to determine the attitude using the optimal attitude matrix. The loss function is defined as [25],

$$L\left(\mathbf{A}\right) = \frac{1}{2}\sum_i a_i \left| \mathbf{b}_i - \mathbf{A}\mathbf{r}_i \right|^2 \tag{3}$$

where $\mathbf{b}_i$ is the measurement vector in the body coordinate system and $\mathbf{r}_i$ is the reference model in inertial frame, $\mathbf{A}$ is the attitude transformation matrix from inertial to body frame, a_i is the non-negative weights of each sensor. The singular value decomposition (SVD) method is one of the single-frame methods (SFMs) used for minimization of Wahba's loss function [26, 27] in determining the attitude of a spacecraft.

Second stage processes the attitude measurements and related covariance matrix in the Kalman-type attitude estimation filter. The state vector can be estimated as,

$$\hat{\mathbf{x}}(k+1) = \hat{\mathbf{x}}(k+1/k) + \mathbf{K}(k+1) \times \left\{ \mathbf{z}(k) - \mathbf{H}\ \hat{\mathbf{x}}(k+1/k) \right\} \tag{4}$$

where $\mathbf{z}(k) = \begin{bmatrix} \mathbf{z}_\Phi(k) & \mathbf{z}_\omega(k) \end{bmatrix}^T$ is the measurement vector of attitude angles and angular velocities respectively, $\mathbf{H}$ is the measurement matrix. For this study, the measurement matrix is a 6x6 unit matrix. The state prediction is,

$$\hat{\mathbf{x}}(k+1/k) = \mathbf{f}\left[\hat{\mathbf{x}}(k), k\right] \tag{5}$$

where $\mathbf{f}\left[\cdot\right]$ is the nonlinear system function. The gain of the filter is,

$$\mathbf{K}(k+1) = \mathbf{P}(k+1/k)\mathbf{H}^T \times \left[\mathbf{H}\ \mathbf{P}(k+1/k)\mathbf{H}^T + \mathbf{R}(k)\right]^{-1} \tag{6}$$

SFM is used in the first stage to determine the attitude measurements contained in $\mathbf{z}$ vector as $\mathbf{z}_{\Phi}$, and update the measurement noise covariance matrix, $\mathbf{R}$ in every step. The attitude measurements of SFM can also be used as initialization values instead of choosing them manually.

The covariance matrix of the prediction error is,

$$\mathbf{P}(k+1/k)=\frac{\partial \mathbf{f}[\hat{\mathbf{x}}(k),k]}{\partial \hat{\mathbf{x}}(k)}\mathbf{P}(k/k)\frac{\partial \mathbf{f}^{T}[\hat{\mathbf{x}}(k),k]}{\partial \hat{\mathbf{x}}(k)}+\mathbf{Q} \tag{7}$$

where $\mathbf{Q}$ is the process noise covariance matrix. The covariance matrix of the estimation error is,

$$\mathbf{P}(k+1/k+1)=\left[\mathbf{I}-\mathbf{K}(k+1)\mathbf{H}\right]\mathbf{P}(k+1/k) \tag{8}$$

In case of a bias type of fault on the magnetometers, a Kalman-based magnetometer calibration algorithm can be designed [28]. The continuous-time state equation of the problem can be defined as,

$$\dot{\mathbf{b}}=\mathbf{u}_{b} \tag{9}$$

where $\mathbf{u}_{b}(k)=\left[u_{b_x}(k)\quad u_{b_y}(k)\quad u_{b_z}(k)\right]^{T}$ is zero-mean white noise. The state equation can be rewritten in discrete time as,

$$\mathbf{b}(k)=\mathbf{b}(k-1)+T_{s}\mathbf{u}_{b}(k-1) \tag{10}$$

where $\mathbf{b}(k)=\left[b_x(k)\quad b_y(k)\quad b_z(k)\right]$ and T_s is the sampling time.

The magnetometer measurements can be modeled as,

$$\mathbf{B}_{m}(k)=\mathbf{A}(k)\mathbf{B}_{o}(k)+\mathbf{b}(k)+\mathbf{v}(k) \tag{11}$$

where $\mathbf{B}_{m}(k)$ is the magnetometer measurement vector, $\mathbf{B}_{o}(k)$ is the reference magnetic field vector, $\mathbf{b}(k)$ is the bias vector on the magnetometer measurements, $\mathbf{v}(k)$ is the measurement noise. The following optimum Kalman filter can be designed to estimate the magnetometer bias,

$$\hat{\mathbf{b}}(k)=\hat{\mathbf{b}}(k-1)+\mathbf{K}_{b}(k)\left[\mathbf{B}_{m}(k)-\hat{\mathbf{b}}(k-1)-\mathbf{A}(k)\mathbf{B}_{o}(k)\right] \tag{12}$$

$$\mathbf{K}_{b}(k)=\mathbf{P}_{b}(k/k-1)\left[\mathbf{P}_{b}(k/k-1)+\mathbf{R}_{v}\right]^{-1} \tag{13}$$

$$\mathbf{P}_{b}(k)=\left[\mathbf{I}-\mathbf{K}_{b}(k)\right]\mathbf{P}_{b}(k/k-1) \tag{14}$$

$$\mathbf{P}_{b}(k/k\text{-}1)=\mathbf{P}_{b}(k\text{-}1)+T_{s}^{2}\mathbf{Q}_{u_b} \tag{15}$$

From this, the biases on each channel of the magnetometer measurements can be estimated for fault compensation in the attitude estimation filter.

4. RESULTS AND DISCUSSION

For the Kalman filter, 1 Hz discretization step is used. The filter has the following properties, initial estimation covariance matrix $\mathbf{P}_0=10\mathbf{I}$, system noise covariance matrix $\mathbf{Q}=0.01\mathbf{I}$, and the measurement noise covariance matrix is directly used from the SVD process as $\mathbf{R}=\mathbf{P}_{SVD}$. The mass moment of inertia of the platform is obtained as $\mathbf{J}=\begin{bmatrix}0.6953 & 0.0160 & -0.0060\\ 0.0160 & 0.6075 & -0.0135\\ -0.0060 & -0.0135 & 1.1724\end{bmatrix}$ $\mathrm{kg\cdot m^2}$ with misalignment from the center of mass as $\begin{bmatrix}dx\\ dy\\ dz\end{bmatrix}=\begin{bmatrix}0.028\\ 0.022\\ 0.017\end{bmatrix}$ mm, and 22.61 kg total mass (they have been calculated in the design stage of the platform with final placement of the masses.).

A. Platform's Maneuverability

The analysis results of a maneuver performed on 30-degree roll and pitch angles are depicted in Figs. 5 and 6. The wheels' maximum speed is set at 9240 RPM, and the limit value is entered in the simulation environment. An attitude input has been given remotely from a computer connected to the platform's computer via Wi-Fi in assessing the maneuver capability of the platform. The air bearing table has then run with this input real-time. For the maneuvers, PD controller is implemented where the desired torque is sent to the reaction wheels on the platform. The control coefficients are adjusted for a 60-second maneuver to minimize wheel saturation and ensure optimal performance. The system reaches a steady state within 60 seconds at initial speeds of 500 RPM, with a maximum speed value of less than 1000 RPM on all three wheels. The wheels remained within the specified torque and angular momentum capacity limits, avoiding the risk of saturation for the next maneuver. The wheels' saturation status is checked for successive maneuvers, as shown in Figs. 7 and 8, and they do not undergo saturation in these maneuvers.

B. Validating the Attitude Estimation and Magnetometer Calibration Algorithms

The attitude estimation algorithm uses magnetometer, angular velocity measurements, and accelerometer measurements to estimate roll, pitch, and yaw angles of a test table in three axes. The estimation algorithm is based on angular velocity data, which are linear measurements.

A conventional attitude estimation method is designed, utilizing both system and sensor measurement models as inputs listed as:

1. The estimated angular velocity values from the previous step,
2. Attitude angle estimated values in the preceding step,
3. Angular velocity measurements,
4. The angular velocity sensor error covariance value,
5. The offset value between the accelerometer's location and the rotation center,
6. Measurements from the accelerometer,
7. Accelerometer error covariance value,
8. Moment of inertia matrix,
9. The offset value between rotation and the mass centers,
10. The system's overall mass,
11. Kalman estimation filter initial covariance matrices (tuning parameters).

For the conventional filter, the accelerometer data read from the sensor is compared with the gravity vector and the angular movement in the horizontal plane could be calculated. These measurements are not used in the SVD-aided EKF algorithm. The theoretical magnetic field model outputs and magnetometer data from the test setup are retrieved. For the theoretical magnetic field model, 13^{th} degree and order of the spherical harmonics is used without any truncation. The SVD-aided EKF then uses the test setup's magnetometer data as well as the model-based sun sensor vector outputs. Solar sensor is modeled theoretically, as the facility does not have a solar simulator yet. More information on SFM-aided Kalman-type filters can be found in [23, 29]. Figure 9 shows the estimation findings as roll, pitch, and yaw angles along the x, y, and z axes, respectively. This test; therefore, to the best of the authors' knowledge, validates the SVD-aided EKF algorithm on the test table experiments, which was presented only theoretically in previous studies.

It is also possible to estimate the bias in the magnetometer measurements. Bias estimation in the augmented states can be used to calibrate magnetometers. For testing the magnetometer calibration algorithm, magnetometer measurements are corrupted by a continuous bias as 2000 nT in x, 3000 nT in y, and 1000 nT in the z-direction. The bias corruption is applied on top of the magnetometer measurement outputs before the filtering stage using the model provided in Equation (9). The calibration of the magnetometer measurements is carried out using a linear Kalman filtering method [28]. The magnetometer

biases are estimated quickly, and the filter converges within 40 seconds, as depicted in Fig. 10. A complementary table is created for assessing the results. Here, Table 1 presents the absolute and relative estimation errors of the magnetometer biases as nT and percentages respectively. After 30 seconds, the errors are approaching zero, confirming the convergence of the estimation.

5. CONCLUSIONS

The structural systems are designed for the attitude determination and control test platform. Sensors and actuators are chosen based on a trade-off when creating the test setup. The platform validates algorithms built for estimating small satellite attitude. This is accomplished through the employment of both classic and non-traditional EKF techniques. For the control method, the well-known PD controller is implemented for assessing the maneuverability capabilities of the platform.

Small low Earth-orbiting satellites primarily utilize magnetometers for attitude state determination due to their lightweight, reliable, and low power consumption properties. Magnetometer bias errors must be adjusted in order to accurately determine the attitude. Magnetometer observations during the initial stages of satellite missions are critical for determination and control systems. In this study, the Kalman filter-based approach is utilized to calculate the bias in each channel of magnetometer measurements.

FUNDING

The work was supported by TUBITAK (The Scientific and Technological Research Council of Turkey), Grant 113E595.

REFERENCES

1. Kramlikh A V., Nikolaev PN, Rylko D V. (2023) Onboard Two-Step Attitude Determination Algorithm for a SamSat-ION Nanosatellite. Gyroscopy and Navigation 14:138–153. https://doi.org/10.1134/s2075108723020050
2. Cilden-Guler D, Hajiyev C (2023) SVD-Aided EKF for Nanosatellite Attitude Estimation Based on Kinematic and Dynamic Relations. Gyroscopy and Navigation 14:366–379
3. Schwartz JL, Peck MA, Hall CD (2012) Historical Review of Air-Bearing Spacecraft Simulators. Journal of Guidance Control and Dynamics 26:513–522. https://doi.org/10.2514/2.5085
4. Al-Majed MI, Alsuwaidan BN (2009) A new testing platform for attitude determination and control subsystems: Design and applications. In: IEEE/ASME International Conference on Advanced Intelligent Mechatronics, AIM. pp 1318–1323
5. Tavakoli A, Faghihinia A, Kalhor A (2017) An innovative test bed for verification of attitude control system. IEEE Aerospace and Electronic Systems Magazine 32:16–22. https://doi.org/10.1109/MAES.2017.150198
6. Cardoso da Silva R, Alves Rodrigues U, Alves Borges R, et al (2016) A test-bed for attitude determination and control of spacecrafts. In: II Latin American IAA CubeSat Workshop. Florianopolis, Brazil
7. Modenini D, Bahu A, Curzi G, Togni A (2020) A Dynamic Testbed for Nanosatellites Attitude Verification. Aerospace 7:31. https://doi.org/10.3390/AEROSPACE7030031
8. Ovchinnikov MY, Ivanov DS, Ivlev NA, et al (2014) Development, integrated investigation, laboratory and in-flight testing of Chibis-M microsatellite ADCS. Acta Astronaut 93:23–33
9. Chen X, Su Z, Wengao L, et al (2016) General-purpose ground test system for the attitude determination and control subsystem of pico/nano-satellite. 2015 IEEE 12th International Conference on Electronic Measurement and Instruments, ICEMI 2015 2:1004–1009. https://doi.org/10.1109/ICEMI.2015.7494373
10. Yavuzyilmaz C, Akbas M, Acar Y, et al (2011) Rasat ADCS flight software testing with dynamic attitude simulator environment. In: Proceedings of 5th International Conference on Recent Advances in Space Technologies (RAST). pp 974–977
11. Tsiotras P, Kriengsiri P (2003) Designing a Low-Cost Spacecraft Simulator. IEEE Control Syst 23:26–37. https://doi.org/10.1109/MCS.2003.1213601
12. Sanders D, Heater D, Peeples SR, et al (2013) Pushing the Limits of Cubesat Attitude Control: A Ground Demonstration. In: Small Satellite Conference
13. Sato Y, Fujita S, Kuwahara T, et al (2017) Improvement and verification of satellite dynamics simulator based on flight data analysis. In: IEEE/SICE International Symposium on System Integration. Institute of Electrical and Electronics Engineers Inc., Taipei, Taiwan, pp 686–691
14. Ousaloo HS, Nodeh MT, Mehrabian R (2016) Verification of Spin Magnetic Attitude Control System using air-bearing-based attitude control simulator. Acta Astronaut 126:546–553. https://doi.org/10.1016/J.ACTAASTRO.2016.03.028

15. Ho MT, Tu YW, Lin HS (2009) Controlling a Ball and Wheel System Using Full-State-Feedback Linearization: A Testbed for Nonlinear Control Design. IEEE Control Syst 29:93–101. https://doi.org/10.1109/MCS.2009.934085
16. Medina I, Santiago L, Hernández-Gómez JJ, et al (2021) Speed PID controller simulation of a reaction wheel for CubeSat orientation applications. J Phys Conf Ser 1723:012013. https://doi.org/10.1088/1742-6596/1723/1/012013
17. Inumoh LO, Forshaw JL, Horri NM (2015) Tilted wheel satellite attitude control with air-bearing table experimental results. Acta Astronaut 117:414–429. https://doi.org/10.1016/j.actaastro.2015.09.007
18. de Melo ACCP, Cafe DC, Alves Borges R (2020) Assessing Power Efficiency and Performance in Nanosatellite Onboard Computer for Control Applications. IEEE Journal on Miniaturization for Air and Space Systems 1:110–116. https://doi.org/10.1109/JMASS.2020.3009835
19. Costa RF, Saotome O, Rafikova E (2019) Simulation and Validation of Satellite Attitude Control Algorithms in a Spherical Air Bearing. Journal of Control, Automation and Electrical Systems 2019 30:5 30:716–727. https://doi.org/10.1007/S40313-019-00497-4
20. Song H, Hu SL, Chen WZ (2021) Simulink-based simulation platform design and faults impact analysis of attitude control systems. The Aeronautical Journal 1–25. https://doi.org/10.1017/AER.2021.79
21. Chen Z, Luo Z, Wu Y, et al (2021) Research on high-precision attitude control of joint actuator of three-axis air-bearing test bed. Journal of Control Science and Engineering 2021:. https://doi.org/10.1155/2021/5582541
22. Kutlu A, Cilden-Guler D, Hajiyev C (2023) A Test-Bed for Attitude Determination and Control System of Nanosatellite. In: Karakoc TH, Yilmaz N, Dalkiran AEAH (eds) New Achievements in Unmanned Systems. Springer, Cham, pp 27–35
23. Hajiyev C, Cilden Guler D (2017) Review on Gyroless Attitude Determination Methods for Small Satellites. Progress in Aerospace Sciences 90:54–66. https://doi.org/10.1016/j.paerosci.2017.03.003
24. Cilden-Guler D, Raitoharju M, Piche R, Hajiyev C (2019) Nanosatellite attitude estimation using Kalman-type filters with non-Gaussian noise. Aerosp Sci Technol 92:66–76. https://doi.org/10.1016/J.AST.2019.05.055
25. Markley FL, Crassidis JL (2014) Fundamentals of Spacecraft Attitude Determination and Control. Springer, New York
26. Wahba G (1965) Problem 65-1: A Least Squares Estimate of Satellite Attitude. Society for Industrial and Applied Mathematics Review 7:409
27. Cilden-Guler D, Conguroglu ES, Hajiyev C (2017) Single-Frame Attitude Determination Methods for Nanosatellites. Metrology and Measurement Systems 24:313–324. https://doi.org/10.1515/mms-2017-0023
28. Hajiyev C (2015) Orbital Calibration of Microsatellite Magnetometers Using a Linear Kalman Filter. Measurement Techniques 58:1037–1043. https://doi.org/10.1007/s11018-015-0838-4
29. Cilden D, Soken HE, Hajiyev C (2017) Nanosatellite attitude estimation from vector measurements using SVD-AIDED UKF algorithm. Metrology and Measurement Systems 24:113–125. https://doi.org/10.1515/mms-2017-0011

TABLES

Table 1. The magnetometer bias estimations (absolute and relative errors)

Time (s)	Absolute Error (nT)			Relative Error $(\%)$		
	x	y	z	x	y	z
10	-5.4249	-8.1374	1.0850	-0.0027	-0.0027	0.0011
20	-1.4951	-2.2428	0.2990	-0.7476e-3	-0.7476e-3	0.2990e-3
30	-0.4452	-0.6679	0.0890	0.2226e-3	0.2226e-3	0.0890e-3
40	-0.1334	-0.2002	0.0267	0.6674e-4	0.6674e-4	0.2669e-4
50	-0.0400	-0.0601	0.0080	0.2002e-4	0.2002e-4	0.0801e-4
60	-0.0120	-0.0180	0.0024	0.6004e-5	0.6004e-5	0.2402e-5

FIGURE CAPTIONS

Fig. 1. Conceptual configuration of equipment put on the platform.

Fig. 2. Assembly of manufactured test table.

Fig. 3. The diagram for the reference frames visualization.

Fig. 4. Attitude determination and control algorithm block schema.

Fig. 5. Maneuver: Attitude states of the platform.

Fig. 6. Maneuver: Angular velocities of the reaction wheels.

Fig. 7. Successive maneuver: Attitude states of the platform.

Fig. 8. Successive maneuver: Angular velocities of the reaction wheels.

Fig. 9. SVD-aided EKF algorithm estimation.

Fig. 10. Mean error of bias estimation.

FIGURES

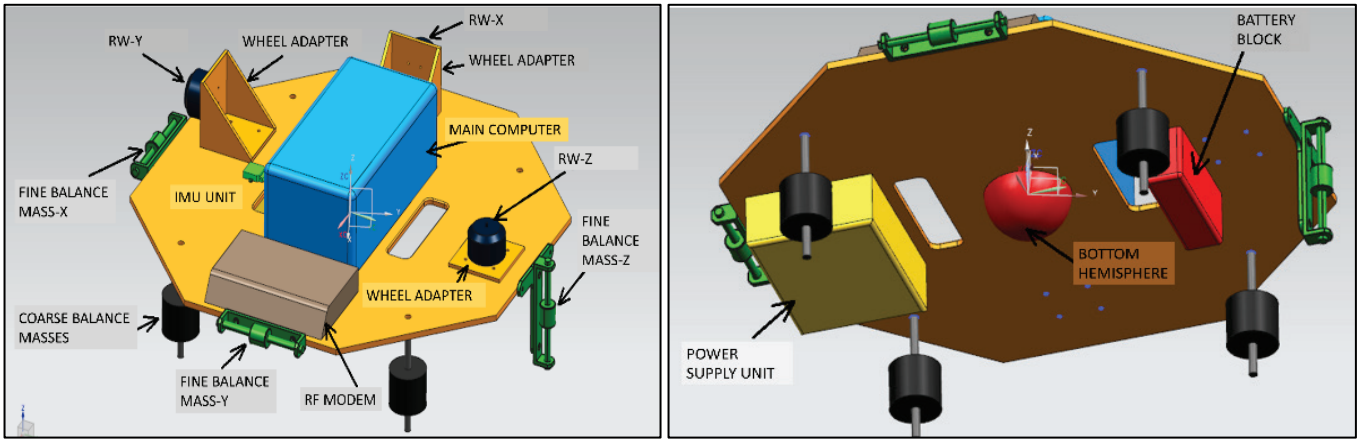

Fig. 1. Conceptual configuration of equipment put on the platform.

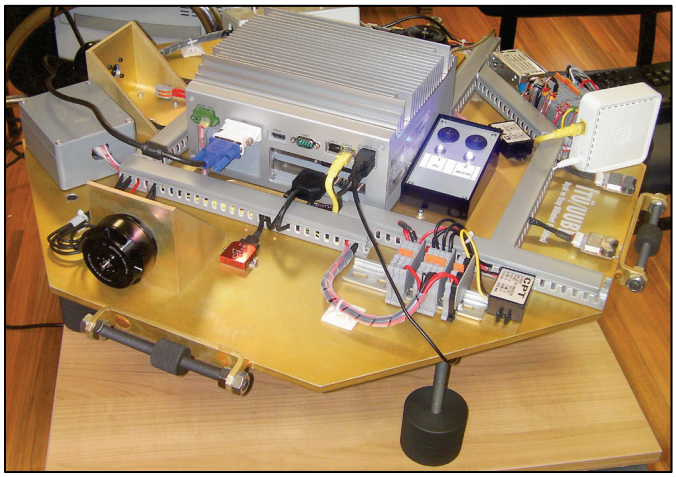

Fig. 2. Assembly of manufactured test table.

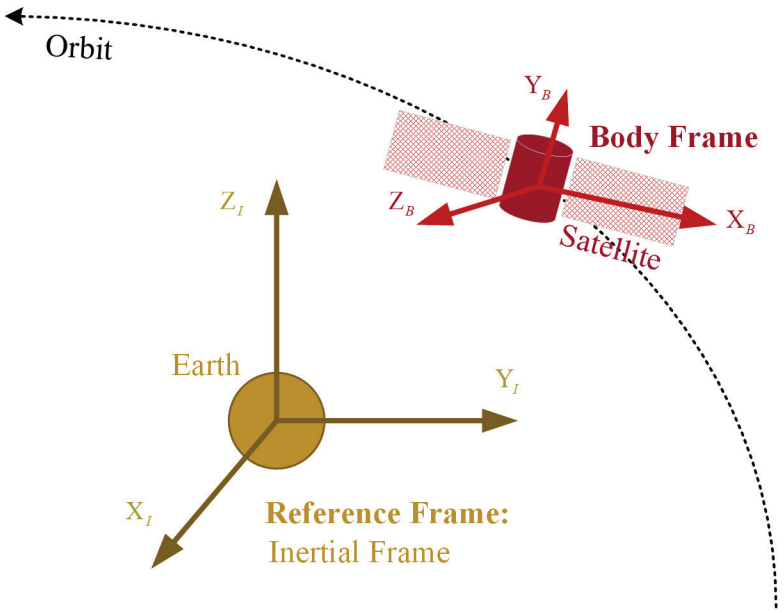

Fig. 3. The diagram for the reference frames visualization.

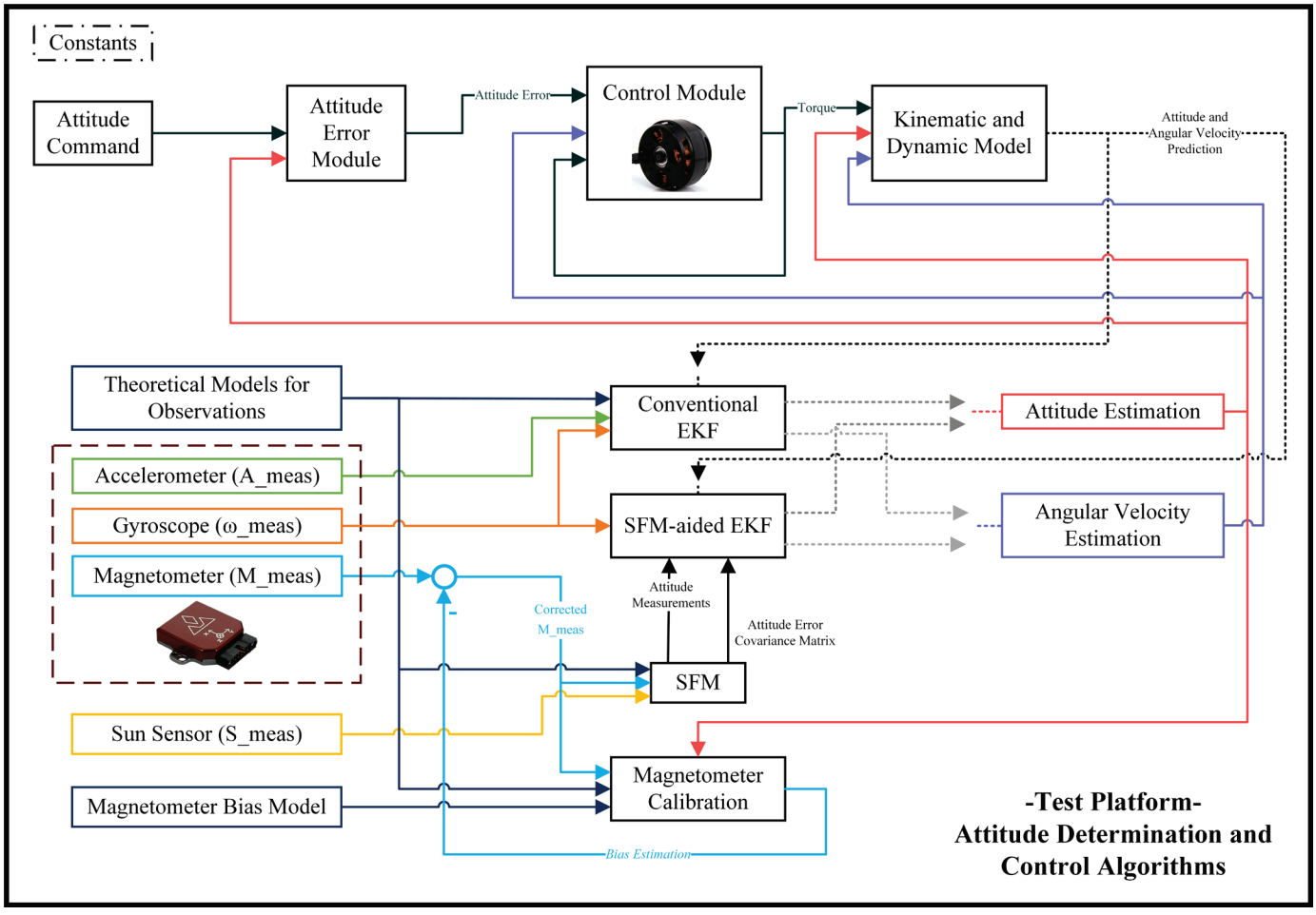

Fig. 4. Attitude determination and control algorithm block schema.

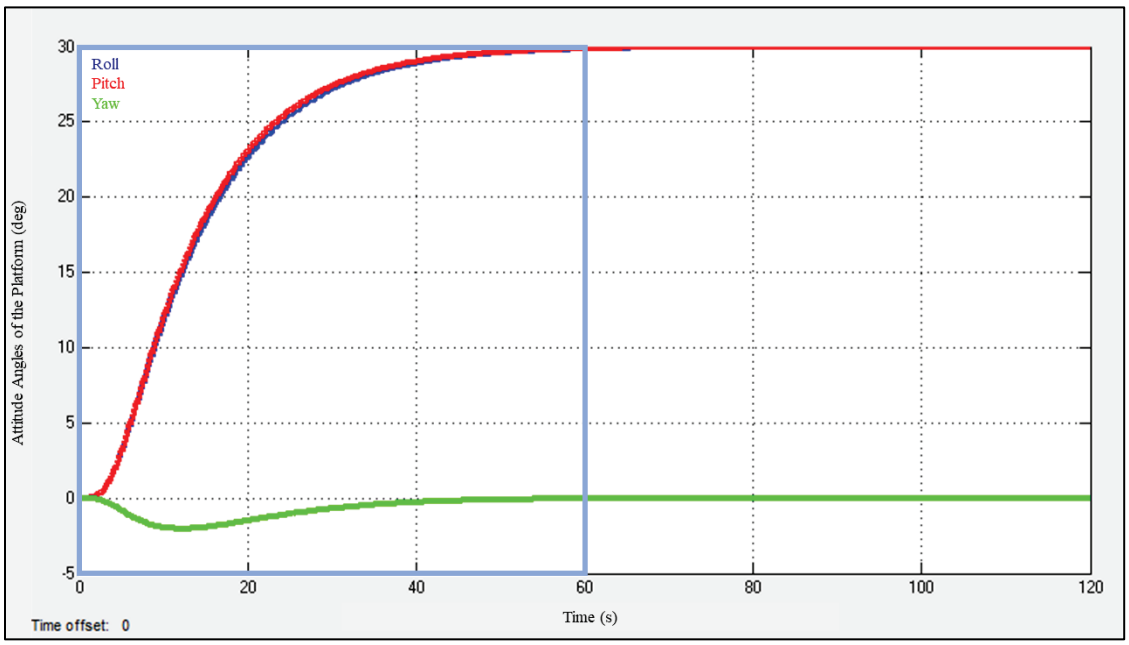

Fig. 5. Maneuver: Attitude states of the platform.

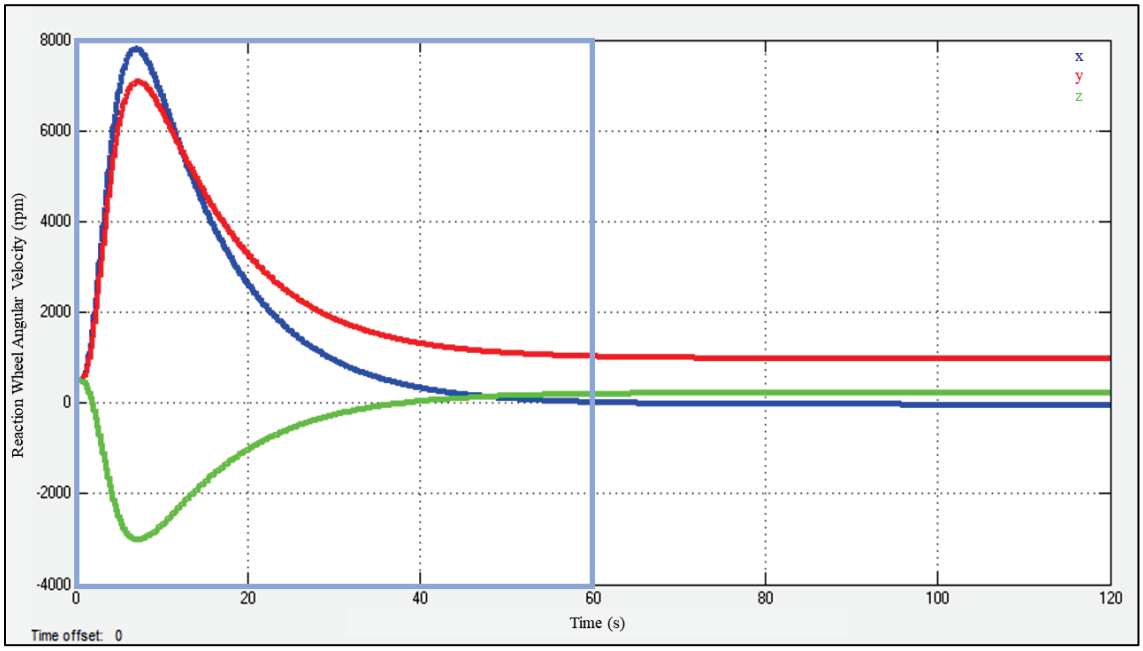

Fig. 6. Maneuver: Angular velocities of the reaction wheels.

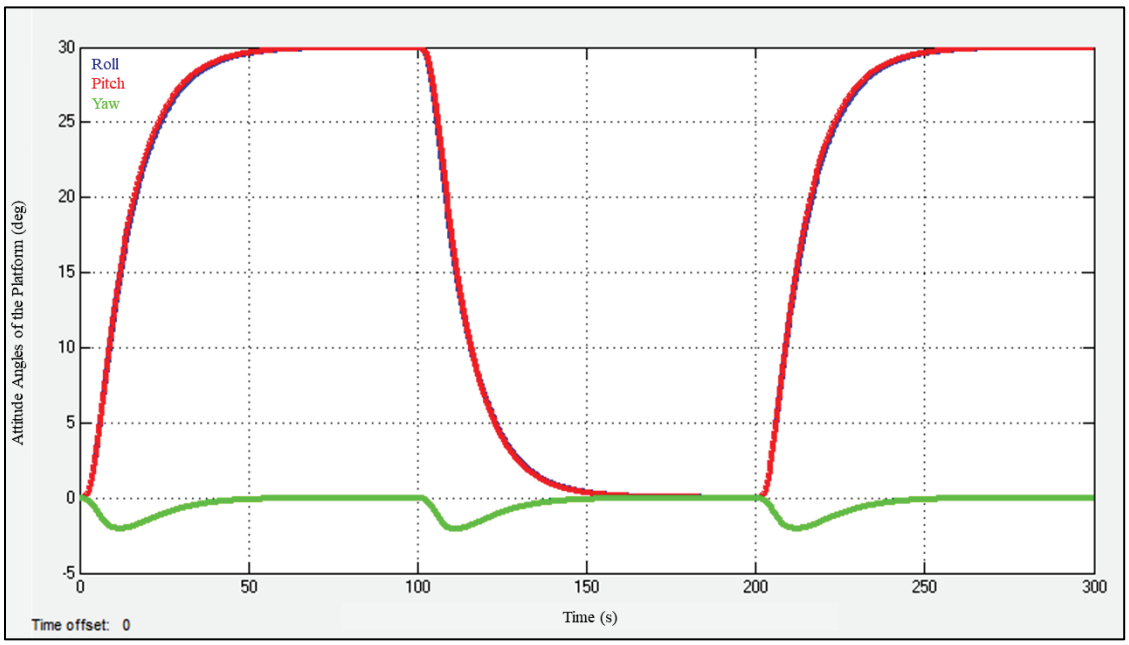

Fig. 7. Successive maneuver: Attitude states of the platform.

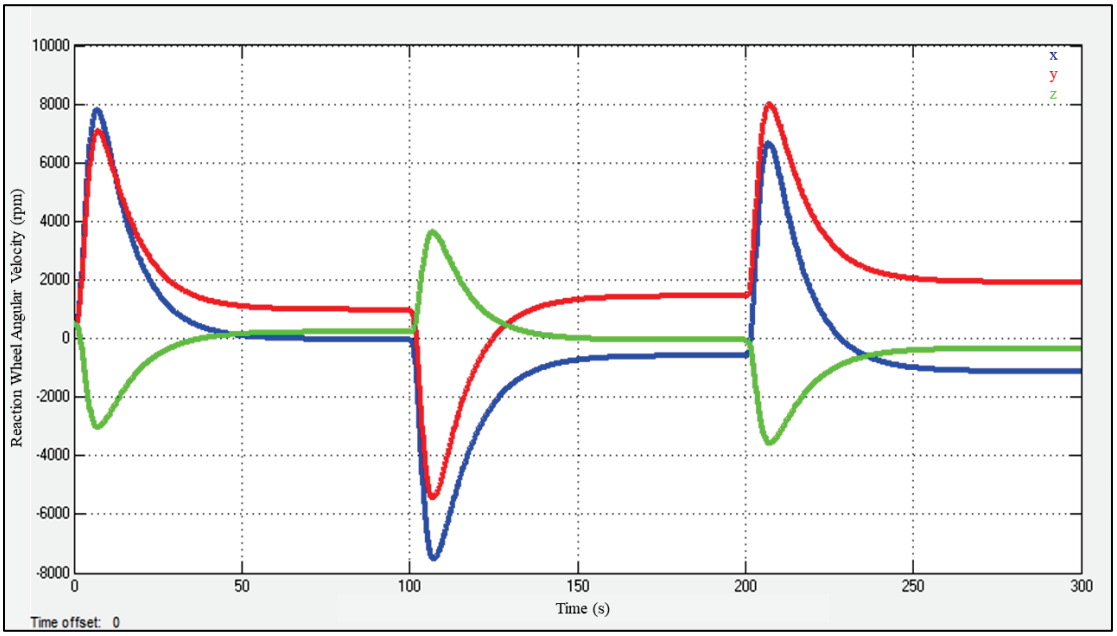

Fig. 8. Successive maneuver: Angular velocities of the reaction wheels.

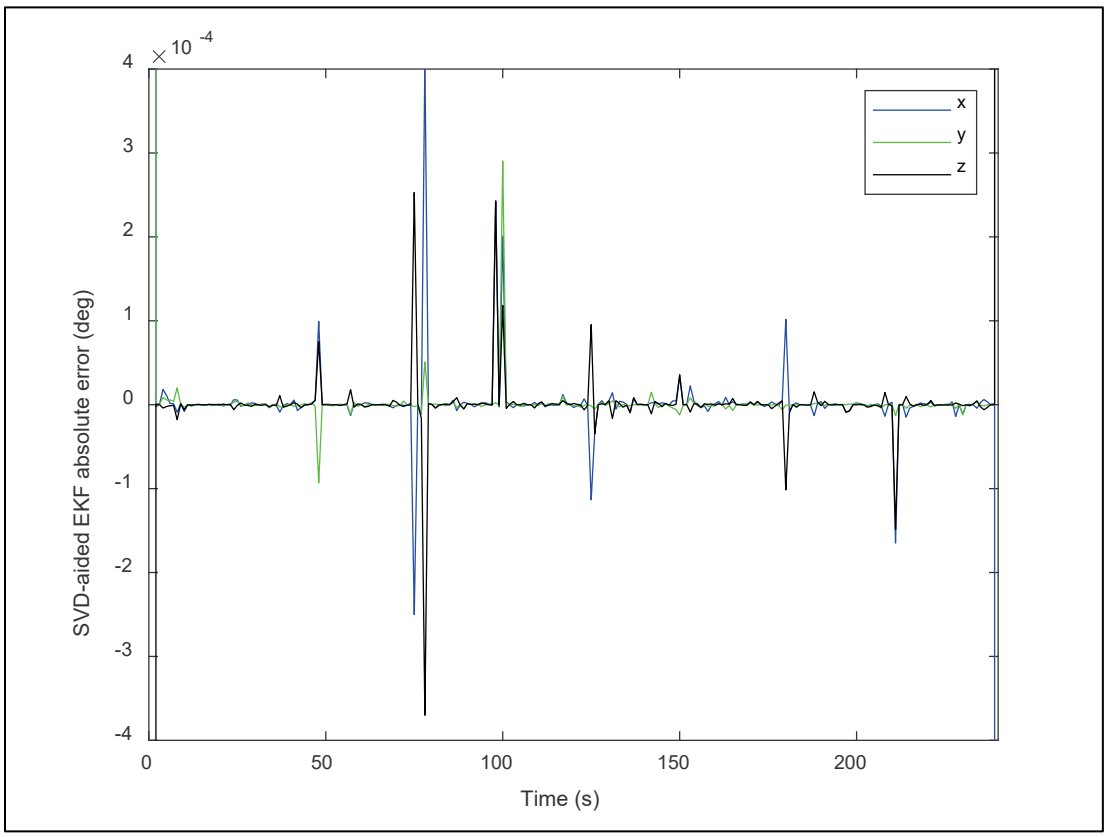

Fig. 9. SVD-aided EKF algorithm estimation.

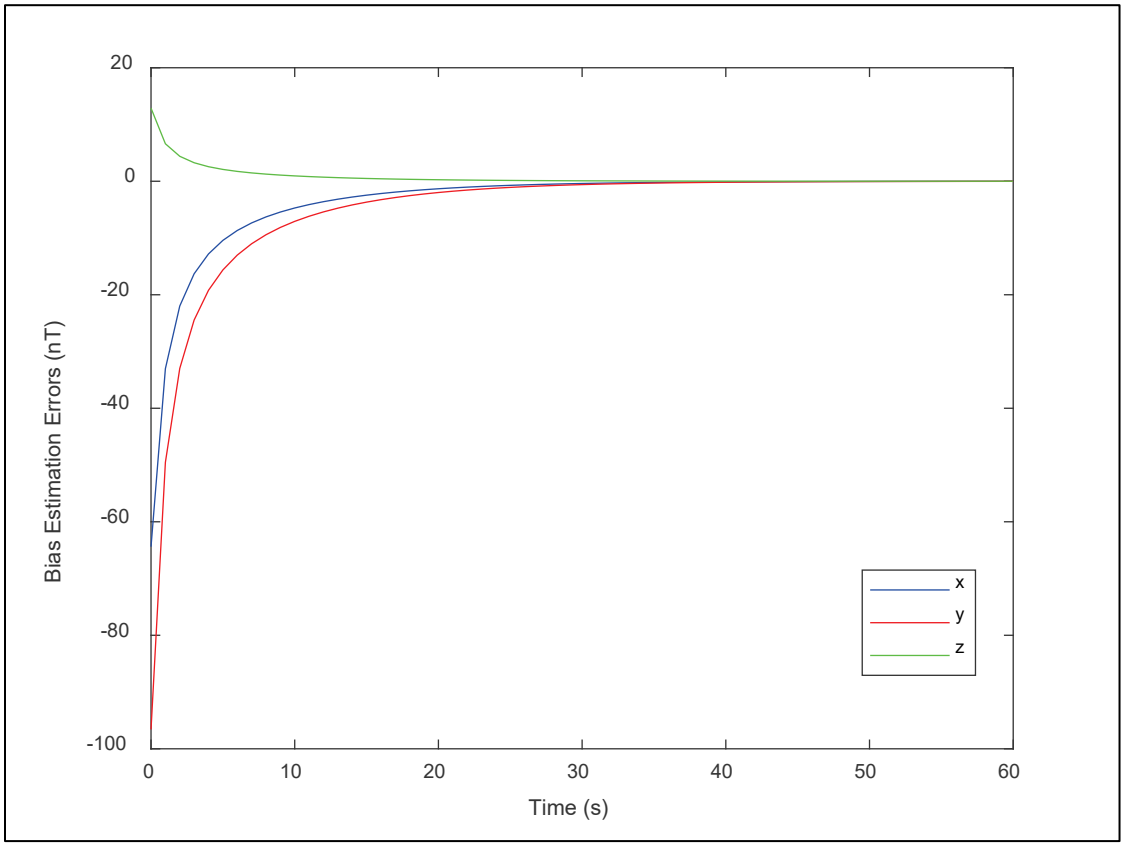

Fig. 10. Mean error of bias estimation.